

Heavy Flavor Measurements in ATLAS and CMS

J. Schieck on behalf of the ATLAS and CMS Collaboration

*Ludwig-Maximilians-Universität München , Am Coulombwall 1, 85748 Garching, Germany and
Excellence Cluster Universe, Boltzmannstrasse 2, 85748 Garching, Germany*

We present heavy flavor measurements performed by the ATLAS and CMS Collaborations with data collected at the Large Hadron Collider. The production mechanism of heavy flavor hadrons is discussed as well as lifetime measurements and searches for the rare decay $B_s^0 \rightarrow \mu^+ \mu^-$. The large available statistics of about 5 fb^{-1} per experiment collected during the year 2011 together with the excellent detector performance allows to perform competitive heavy flavor measurements.

1 Introduction

The production and the decay of hadrons containing a b-quark provide an excellent laboratory to study the strong as well as the weak interaction of the Standard Model of Particle Physics. The large b-quark production cross-section in proton-proton collisions at the Large Hadron Collider (LHC) offers the possibility of performing heavy flavor measurements with an unprecedented statistical accuracy. Here we present heavy flavor results obtained with data taken by the ATLAS¹ and CMS² detectors in the year 2010 and 2011.

In section 2 we will describe the experimental setup together with the collected data used by the measurements, in section 3 B-hadron production measurements are summarized, in section 4 lifetime measurements are discussed and finally in section 5 the search for the rare B-hadron decay $B_s^0 \rightarrow \mu^+ \mu^-$ is presented. We conclude with a summary in section 6.

2 Experimental Setup

Both ATLAS and CMS are designed as multi-purpose experiments, focusing mainly on searches for new physics phenomena at large transverse momentum scales. Both experiments cover a rapidity range up to $|\eta| < 2.5$. However, the bulk of the b-quark production peaks at large rapidities and both experiments are only able to collect a fraction of the produced B-hadrons. The main sub-detectors used for heavy-flavor measurements are the tracking devices located closest to the interaction point and the muon-detectors, the sub-detector farthest out. The muon detectors are used to identify and to trigger on muon decays of B-hadrons. The tracking devices consist of high precision silicon detectors, and they are used to reconstruct the production and the decay vertices of B-hadrons. The large boost of high momentum B-hadrons leads to secondary decay vertices dislocated up to several millimeters from the primary production vertex. The tracker and the muon systems are placed in a large magnetic field to determine the momentum of the charged tracks with high accuracy, leading to a concomitantly high mass resolution. Fig. 1 shows the invariant mass distribution of J/ψ candidates decaying into two muons being

reconstructed in the barrel region of the ATLAS detector³ and the CMS detector⁴. The mass resolution is determined to be between $\sigma = 46$ to 111 MeV (ATLAS) and between $\sigma = 20$ and 50 MeV (CMS), broadening with increasing rapidity. The high mass resolution is important to reach a good signal to background ratio for reconstructed B-hadron candidates. The impact parameter resolution is determined by the single hit resolution of the tracking devices and is limited by multiple scattering effects of low momentum tracks. For any measurement using lifetime based quantities the impact parameter measurement is a crucial ingredient.

It should be noted that both detectors have only very limited particle identification possibilities. Only the silicon tracking devices have some kaon-pion separation power in the momentum region below one GeV/c . Above one GeV/c no kaon-pion separation is possible, leading to increased background conditions for reconstructed B-hadron candidates with kaons in the final state. The muon detectors are essential for selecting B-hadron events. Since tracking devices are not part of the first trigger decision, B-hadron decays with leptons in the final state are used to select B-hadron events. The most promising possibility offer B-hadron decays with two oppositely charged muons in the final state like the decay into a J/ψ or B-hadron decaying directly into a pair of muons. However, the overall trigger rate with two muon candidates in the final state exceeds the limits imposed by both the trigger itself and the long-term data storage resources, so this must be mitigated by applying trigger pre-scales or by raising the momentum thresholds for the candidates (with a preference for the latter). Overall the ATLAS detector collects 5.25 fb^{-1} and the CMS detector 5.56 fb^{-1} of data in 2011 with a maximum instantaneous luminosity of $\sim 3.5 \times 10^{33} \text{ cm}^{-2} \text{ s}^{-1}$. For this luminosity the setup of the accelerator induces on average up to 11.6 collisions per bunch crossing, a challenge for any heavy flavor physics measurement.

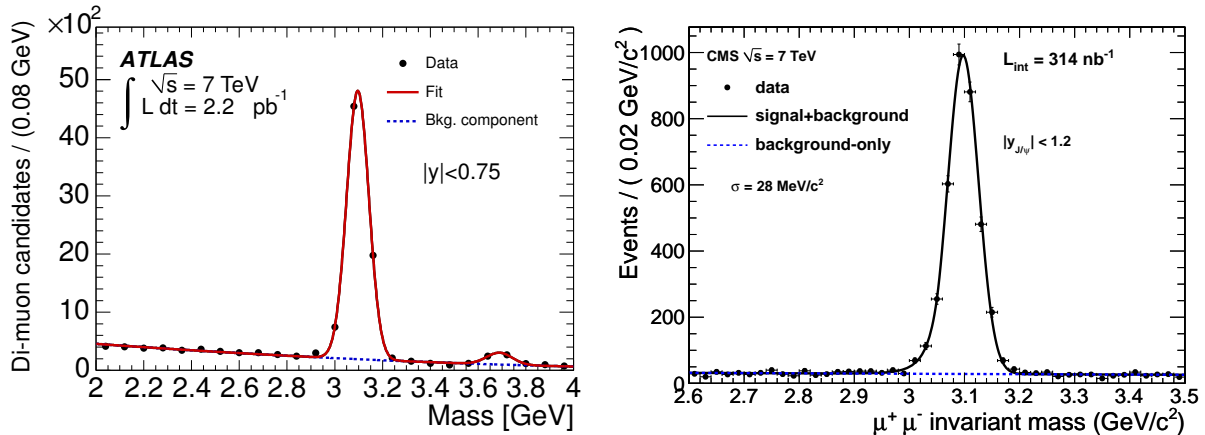


Figure 1: J/ψ candidates reconstructed in the barrel region of the ATLAS detector (left)³ and of the CMS detector (right)⁴.

3 B-Hadron Production

In a hadron collider such as the LHC the bulk of b-quarks and the following B-hadrons are produced via the strong interaction. The production mechanism can be described in the context of perturbative and non-perturbative Quantum Chromo Dynamics (QCD) and a measurement of the B-hadron production rate offers an excellent test of QCD models. Besides the production of B-hadrons the generation of quarkonium states like the $\Upsilon(1S)$, $\Upsilon(2S)$, $\Upsilon(3S)$, the J/ψ and the $\psi(2S)$ are also of great interest. Quarkonium production measurements can be used to probe the mechanism of $q\bar{q}$ -generation followed by the subsequent evolution of the quark pair into a quarkonium state⁵. However, B-hadron decays and higher mass charmonium states like the χ_c

will contribute to the overall non-prompt charmonium production rate.

3.1 Quarkonium Production and Observation of a new χ_b State

Precise measurements of quarkonium production are performed by the ATLAS and the CMS Collaborations. Both collaborations measure the charmonium production rate and compare it to various theoretical predictions. The CMS Collaboration⁶ studies the prompt and non-prompt production rate of J/ψ and $\psi(2S)$ as a function of p_T and rapidity. The data sample corresponds to an integrated luminosity of 37 pb^{-1} . The prompt (non-prompt) production rate is compared to NLO NRQCD (FONLL) theory predictions. All measurements are in agreement with the theory predictions. The agreement found for the prompt $\psi(2S)$ production rate is of particular interest since no feed-down from higher mass charmonium states is expected and therefore a direct comparison to the theory prediction is possible. The differential production rate of the prompt $\psi(2S)$ production rate as a function of p_T in several rapidity bins is shown in Fig. 2. The ATLAS Collaboration measures the prompt and non-prompt J/ψ production

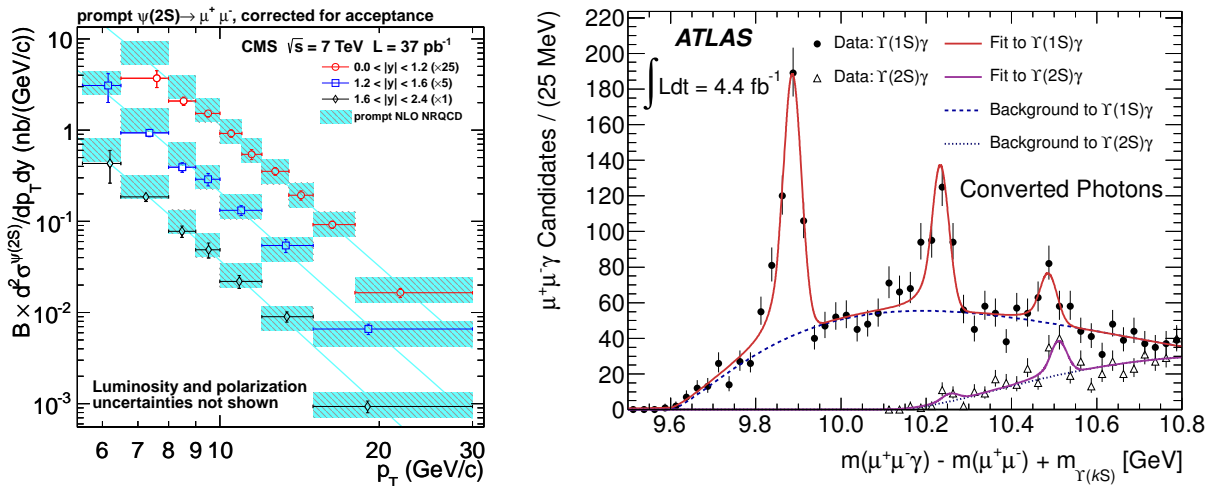


Figure 2: The measured differential cross section as measured by the CMS Collaboration is shown in the left plot for prompt $\psi(2S)$ as a function of p_T and for different rapidity bins⁶. The right plot shows the mass distribution of $\chi_b \rightarrow \Upsilon(k\bar{s})\gamma$ ($k=1,2$) candidates reconstructed with the ATLAS detector with the photon being converted and reconstructed by two electrons⁹. The circles show the data for the χ_b decaying into a $\Upsilon(1S)$ and a photon and the triangles correspond to the χ_b decaying into a $\Upsilon(2S)$ and a photon.

rate (using 2.3 pb^{-1} of data) as a function of p_T and compares the prompt production rate to a simple color evaporation model and NLO and partial NNLO color singlet models (CSM)³. The partial NNLO CSM shows a significant improvement in describing the p_T dependence and the normalization of the prompt production rate, however, differences are still visible. The ATLAS Collaboration performs a measurement of the $\Upsilon(1S)$ production cross section based on 1.13 pb^{-1} of data⁷. The $\Upsilon(1S)$ production rate is dominated by prompt production and contributions from higher mass decays are negligible. The differential production rate as a function of p_T is compared to a NLO CSM with direct contributions only, and to a NRQCD model implemented in PYTHIA 8. The data exceeds significantly the NLO CSM, similar to the charmonium case, which could be explained by the need for higher order corrections. The agreement with the NRQCD predictions are reasonable, but differences up to a factor of two are observed. The CMS Collaboration measures with 3.1 pb^{-1} of integrated luminosity the total and differential production cross section of the $\Upsilon(1S)$, $\Upsilon(2S)$ and the $\Upsilon(3S)$ ⁸ and comparisons to predictions from PYTHIA are performed. The normalized differential cross section with respect to p_T obtained with PYTHIA is consistent with the measurements, while the overall

cross section is overestimated.

The ATLAS Collaboration reports on the observation of a new χ_b state in its radiative transition to $\Upsilon(1S)$ or $\Upsilon(2S)$ ⁹ using an integrated luminosity of 4.4 fb^{-1} . The bottomonium states $\chi_b(1P)$ and $\chi_b(2P)$ are previously observed experimentally and the existence of the $\chi_b(3P)$ state is expected. ATLAS reconstructs the $\chi_b(3P)$ radiative decays from the photon emitted during the transition, and the subsequent decay of the $\Upsilon(1S)$ or $\Upsilon(2S)$ into two muons. The photon is either reconstructed directly in the electromagnetic calorimeter or via two electrons originating from the conversion of the photon. The reconstructed mass of $m_{\chi_b(3P)} = 10.530 \pm 0.005 \text{ (stat.)} \pm 0.009 \text{ (syst.)} \text{ GeV}$ is consistent with the expectation from theoretical models averaging the mass over the three $\chi_b(3P)$ hyperfine triplet states. The mass distribution of the $\chi_b \rightarrow \Upsilon(\text{ks}) \gamma$ ($k=1,2$) candidates with the photon reconstructed via photon conversion is shown in Fig. 2.

3.2 B-Meson and B-Baryon Production

The CMS Collaboration measures the total cross section of the B^\pm -meson, B^0 -meson and B_s^0 -meson using exclusively reconstructed decay channels $B^\pm \rightarrow J/\psi K^\pm$ (using 5.8 pb^{-1}), $B^0 \rightarrow J/\psi K_s^0$ and $B_s^0 \rightarrow J/\psi \phi$ (both using 40 pb^{-1})^{10,11,12}. Besides the total cross section the differential production cross section is determined as a function of the transverse momentum p_T and the rapidity of the B-meson. The measured cross sections are compared to MC@NLO and PYTHIA Monte Carlo predictions. For all three cross section measurements the theoretical prediction by MC@NLO is below the measured value while the PYTHIA prediction is above the measured one. The rapidity dependence observed in data is flatter than predicted by PYTHIA. The p_T spectrum falls slightly faster than predicted by MC@NLO. A summary of the total cross section measurements and a comparison to MC@NLO is summarized in Fig. 3. CMS also

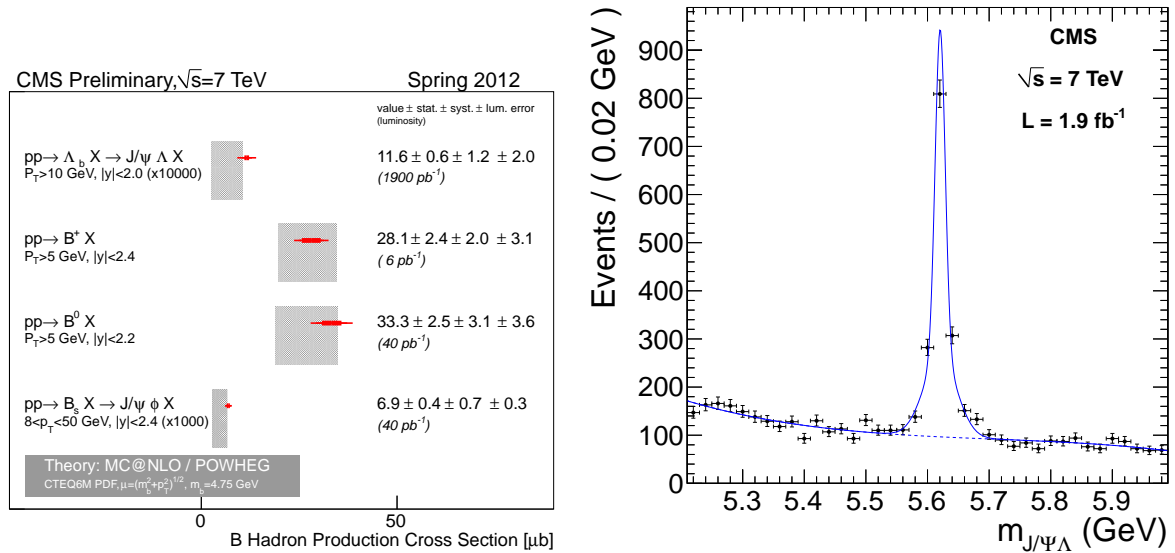


Figure 3: The B-meson cross section measurements performed by the CMS Collaboration are summarized and compared to theory predictions (MC@NLO) in the left figure. The inner error bar corresponds to the statistical uncertainty, the outer error bar to the quadratic sum of statistical and systematic uncertainty. The outermost bracket is the total uncertainty, including the luminosity uncertainty. The invariant mass distribution of the Λ_b reconstructed in the decay $\Lambda_b \rightarrow J/\psi \Lambda$ is shown on the right¹³. The selected Λ_b candidates are reconstructed with a p_T larger than $10 \text{ GeV}/c$ and a rapidity smaller than two.

releases a new measurement of the Λ_b production cross section in pp-collisions at 7 TeV using an integrated luminosity of 1.9 fb^{-1} ¹³. The invariant mass distribution of the Λ_b exclusively

reconstructed with the decay $\Lambda_b \rightarrow J/\psi \Lambda$ is shown in Fig. 3. The cross section measurement is compared to a prediction from PYTHIA. The production rate as a function of the rapidity as well as the ratio $\bar{\Lambda}_b/\Lambda_b$ is well reproduced by PYTHIA. The p_T spectrum of the Λ_b falls faster than the observed meson production, triggering the question as to whether there is a p_T dependent hadronization effect in the ratio of baryon to meson production. A comparison of the p_T spectrum of the b-mesons and the Λ_b -baryon is summarized in Fig. 4. The CMS Collaboration also presents a measurement of the inclusive b-jet production rate at the LHC¹⁴. The results are consistent with the production rate measured by ATLAS and the Monte Carlo predictions using MC@NLO. The inclusive b-jet production rate is shown in Fig. 4.

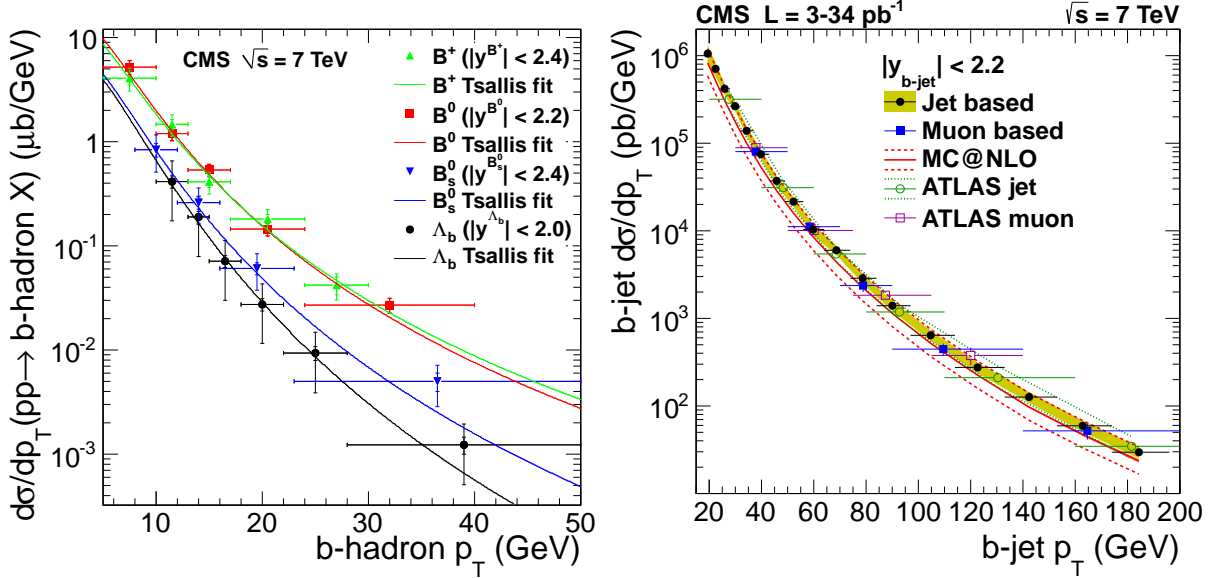


Figure 4: The distribution on the left shows the differential cross section versus p_T reconstructed for the exclusive decays of the B^\pm -meson, B^0 -meson and B_s^0 -meson and the Λ_b -baryon¹³. On the right the inclusive b-jet production rate measured by the ATLAS and CMS Collaboration together with a comparison to MC@NLO is shown¹⁴.

4 Lifetime Measurements

The excellent performance of the tracking devices allows precise measurements of the lifetime of B-hadrons. Besides the measurement of the average B-hadron lifetime a time dependent angular analysis of the decay $B_s^0 \rightarrow J/\psi \phi$ allows a measurement of the B_s^0 -lifetime difference $\Delta\Gamma_s$ of the heavy and light mass eigenstate of the B_s^0 meson. The ATLAS Collaboration presents a measurement of the average B-hadron lifetime using the data taken in 2010, which corresponds to about 40 pb^{-1} ¹⁵. The average B-hadron lifetime is determined via the B-hadron decaying into a $J/\psi + X$, with the J/ψ subsequently decaying in a pair of muons. The decay length of the J/ψ is reconstructed and a correction factor is applied to deduce the lifetime of the parent B-hadron. The correction factor is determined from simulated events, weighted to match the measured J/ψ momentum distribution. The average B-hadron lifetime is measured to be $\langle \tau_b \rangle = 1.489 \pm 0.016(\text{stat.}) \pm 0.043(\text{syst.}) \text{ ps}$. The systematic uncertainty is dominated by the lifetime model of the background events and the alignment uncertainty of the tracking detector.

A measurement of the average lifetime of the B_s^0 meson using exclusively reconstructed $B_s^0 \rightarrow J/\psi \phi$ decays is carried out as well, using the same integrated luminosity of 40 pb^{-1} ¹⁶. Overall 463 ± 26 signal events are reconstructed with estimated 714 ± 38 background events. The single lifetime is measured to be $\tau_{B_{s,\text{single}}} = 1.41 \pm 0.08(\text{stat.}) \pm 0.05(\text{syst.}) \text{ ps}$. Similar to the average lifetime measurement the systematic uncertainty is dominated by the lifetime model

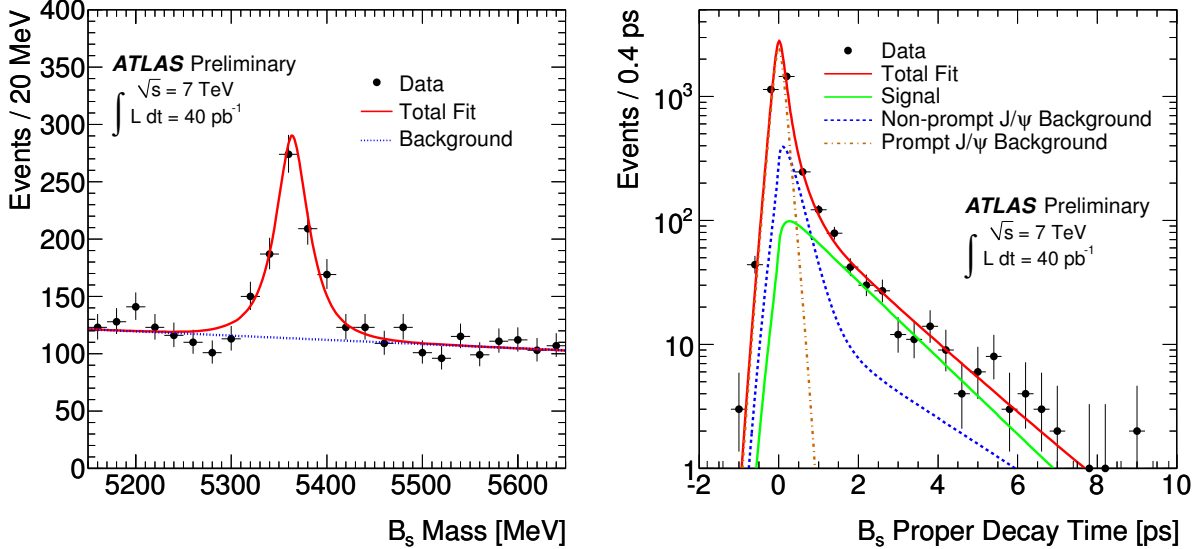


Figure 5: The left plot shows the mass distribution of the reconstructed $B_s^0 \rightarrow J/\psi \phi$ events¹⁶. The right plot shows the lifetime distribution¹⁶. The solid lines are the projections of a simultaneous fit to the mass and lifetime distribution, with the red line reflecting the total fit, the dotted blue line the background contribution and the green line corresponds to the lifetime distribution of signal events. The red dash-dotted line is the contribution from prompt J/ψ events.

of the background as well as the alignment uncertainty of the tracker. Fig. 5 shows the mass and the lifetime distribution of the reconstructed $B_s^0 \rightarrow J/\psi \phi$ events. In both cases the precision of the lifetime measurement is limited by the incomplete knowledge of the tracking detector alignment. It is expected that with increasing statistics and improved knowledge of the tracking devices the uncertainty will decrease significant. The single lifetime measurement of the using $B_s^0 \rightarrow J/\psi \phi$ events is an important step towards the measurement of the weak phase ϕ_s and the lifetime difference $\Delta\Gamma_s$.

5 Rare Decays

The study of rare decays like $B^0 \rightarrow \mu^+ \mu^-$ and $B_s^0 \rightarrow \mu^+ \mu^-$ offers the possibility to searching for physics beyond the Standard Model. This approach is an alternative way to the direct searches performed at ATLAS and CMS selecting high p_T events. Theoretical calculations predict a branching ratio of $3.5 \pm 0.3 \times 10^{-9}$ for the decay $B_s^0 \rightarrow \mu^+ \mu^-$. The ATLAS, CMS and LHCb Collaborations present new measurements on rare B-hadron decays^{19,17,18}. The analysis performed by CMS and LHCb use the complete data set collected in 2011 and are discussed in a separate presentation. In this paper the focus will be on the ATLAS measurement searching for the rare decay $B_s^0 \rightarrow \mu^+ \mu^-$ using data taken with the ATLAS experiment in 2011. Since the trigger conditions changed during the data taking in 2011 the analysis is performed with 2.4 fb^{-1} of collected data only. The branching ratio is not determined directly, but by measuring the ratio to a more abundant B-hadron decay $B^\pm \rightarrow J/\psi K^\pm$. The efficiency, acceptance and the hadronization probability for a b-quark transforming to a B-hadron is different for both decays. The differences are estimated using simulated and data events and the branching ratio $B_s^0 \rightarrow \mu^+ \mu^-$ is finally determined by using the measured ratio. Signal events are separated from background events using a multivariate classifier with 14 discriminating variables. During data taking the event characteristics changed significantly, in particular the number of reconstructed primary vertices per bunch crossing. The left plot of Fig. 6 shows the efficiency dependence

of one of the discriminating variables, the isolation cut which described the activity around a selected B -hadron candidate, as a function of reconstructed primary vertices. After assigning the tracks to the primary vertex the efficiency shows no dependency on the number of reconstructed primary vertices. This clearly shows that this search for rare decays can be still performed with increased instantaneous luminosity. Four out of these 14 discriminating variables are used to optimise the multivariate selection. Two main sources of background events are expected - a continuum background, which is expected to have a smooth dependence on the invariant di-muon mass and a resonant background of mis-reconstructed events, peaking in the same mass range as the signal events. The continuum background can be estimated from the mass sidebands, while the background originating from mis-reconstructed events is estimated using simulated events. The overall background is dominated by the continuum background. The mass resolution varies between candidates with both muons reconstructed in the barrel region of the detector and candidates with at least one muon reconstructed in the forward region of the detector. In order to take this effect into account, the search is divided into three candidate categories depending on the direction of the most forward muon. The selection optimization and the background estimate from sideband events is performed with different event samples. This choices guarantees a bias free estimate of the expected events in the signal region. In total 6.4 events are expected while three events are selected after the search region is unblinded. The right plot in Fig. 6 shows the number of observed and estimated candidates in the sideband and in the signal region. The number of estimated background events and the number of observed signal events together with the event reconstruction efficiency, the acceptance and the hadronization efficiency is used to calculate the upper limit of the branching ratio. The expected 95% confidence limit is $2.3^{+0.9}_{-0.5} \times 10^{-8}$ and the observed one is 2.2×10^{-8} .

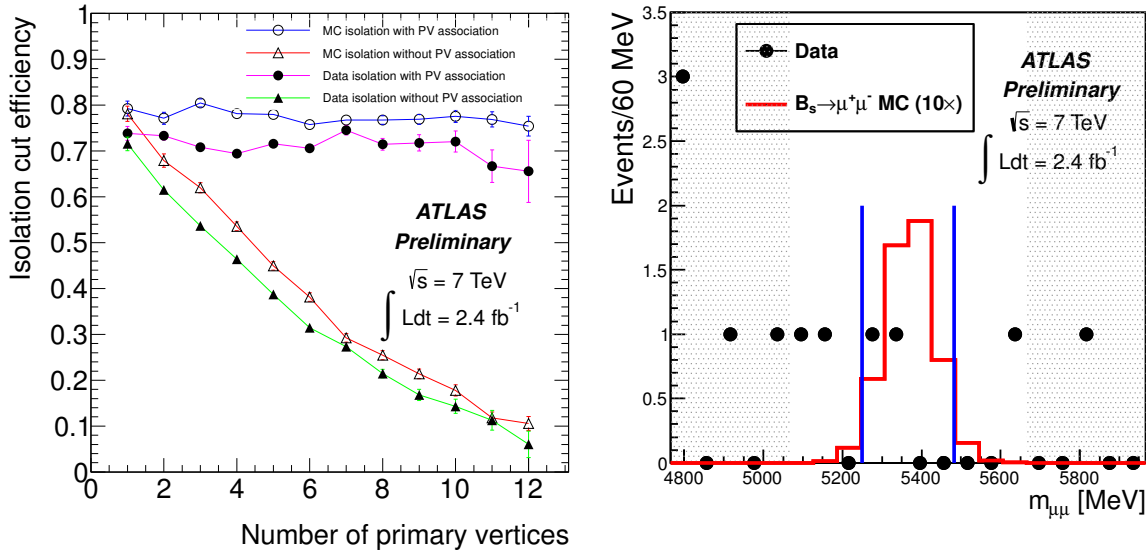


Figure 6: The left plot shows the isolation cut efficiency as a function of reconstructed primary vertices ¹⁹. The triangles show the efficiency for data (closed) and simulated events (closed) not associating the events to the primary vertex as a function of reconstructed primary vertices. Using the primary vertex information the isolation cut efficiency is independent of the number of reconstructed primary vertices, for data (close circles) as well as for simulated events (open circles). The right plot shows the number of reconstructed candidates as a function of the invariant mass, where both muons are reconstructed in the barrel region of the detector ¹⁹. The blue line indicate the signal region, the grey area corresponds to the sideband and the red histogram indicates the expected number of signal events multiplied by a factor of ten.

6 Summary and Conclusion

We report on heavy flavor measurements using data taken in 2010 and 2011 by the ATLAS and the CMS experiment. The large available data set of more than 5 fb^{-1} per experiment and the excellent detector performance allows each to perform many competitive measurements. The measurements of heavy quark production cross sections allow precision studies of QCD. Studies with heavy quarkonium states like the charmonium states J/ψ and $\psi(2S)$ and the bottomonium state $\Upsilon(1S)$, $\Upsilon(2S)$ and $\Upsilon(3S)$ are presented. The measurements are compared to theory models and in several cases large deviations are found. A new bottomonium state, the $\chi_b(3P)$, is observed for the first time by the ATLAS experiment. The CMS Collaboration studies the production of b-flavored hadrons and differences to theory predictions for the total as well as differential production cross section are found. The ATLAS Collaboration presents an average B-hadron lifetime as well as a lifetime measurement using exclusive $B_s^0 \rightarrow J/\psi \phi$ decays. These measurements reflect the good detector performance and are important towards lifetime dependent studies, like the measurement of the weak mixing phase ϕ_s . For the first time ATLAS presents a search for the rare decay $B_s^0 \rightarrow \mu^+ \mu^-$. The number of reconstructed events is consistent with background events only and a 95% confidence limit for the branching ratio is set to 2.2×10^{-8} .

Acknowledgments

This research was supported by the DFG cluster of excellence 'Origin and Structure of the Universe'.

References

1. ATLAS Collaboration, JINST **3** (2008) S08003.
2. CMS Collaboration, JINST **3** (2008) S08004.
3. ATLAS Collaboration, Nucl. Phys. B **850** (2011) 387.
4. CMS Collaboration, Eur. Phys. J. C **71** (2011) 1575.
5. N. Brambilla, S. Eidelman, B. K. Heltsley, R. Vogt, G. T. Bodwin, E. Eichten, A. D. Frawley and A. B. Meyer *et al.*, Eur. Phys. J. C **71**, (2011) 1534.
6. CMS Collaboration, JHEP **1202** (2012) 011.
7. ATLAS Collaboration, Phys. Lett. B **705** (2011) 9.
8. CMS Collaboration, Phys. Rev. D **83** (2011) 112004.
9. ATLAS Collaboration, Phys. Rev. Lett. **108** (2012) 152001.
10. CMS Collaboration, Phys. Rev. D **84** (2011) 052008.
11. CMS Collaboration, Phys. Rev. Lett. **106** (2011) 252001.
12. CMS Collaboration, Phys. Rev. Lett. **106** (2011) 112001.
13. CMS Collaboration, CERN-PH-EP-2012-124 .
14. CMS Collaboration, arXiv:1202.4617 [hep-ex].
15. ATLAS Collaboration, ATLAS-CONF-2011-145, <http://cdsweb.cern.ch/record/1389455>.
16. ATLAS Collaboration, ATLAS-CONF-2011-092, <http://cdsweb.cern.ch/record/1363779>.
17. CMS Collaboration, arXiv:1203.3976 [hep-ex].
18. LHCb Collaboration, arXiv:1203.4493 [hep-ex].
19. ATLAS Collaboration, arXiv:1204.0735 [hep-ex].